IEEE Sensors Council NAL, VOL. XX, NO. XX, MONTH X, XXXX 1

A Roadmap for Electrical Impedance Spectroscopy for Sensing: A Tutorial

Lorenzo A. Buscaglia, Osvaldo N. Oliveira Jr., and J. P. Carmo

***Abstract*—Electrical impedance spectroscopy has been used extensively for sensing and biosensing due to the multiple electrical properties that can be interrogated through varying the frequency of the electrical excitation. In this paper, we review the basic concepts and key issues for applying impedance spectroscopy in sensing and biosensing, with emphasis on the development of precise, low-cost and portable instruments. An impedance spectroscopy system can be divided into three parts: the signal processing unit, the sensing unit and the data analysis unit. Herein, we focus on the signal processing unit, responsible for generating the excitation signal and performing the impedance readout. Special attention is given to small and low-cost signal processing circuits, which are essential for portability and point-of-care diagnosis. We also elaborate upon the various methods to fabricate the sensing units, including the choice of nanomaterials and biomolecules in controlled molecular architectures. From an instrumentation perspective, we discuss possible sources of interference in the measurement protocols. Considerable amounts of data are generated when impedance spectroscopy is utilized with arrays of sensing units, as in electronic tongues, and in surveillance and monitoring systems. This has motivated an increasing use of statistical and computational methods for data analysis. We present some of these methods, with examples of information visualization and machine learning techniques, which have been employed in analyzing impedance spectroscopy data in recent years.**

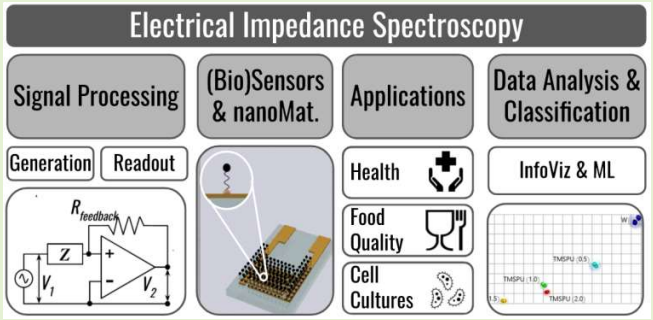

***Index Terms*—impedance spectroscopy, review, signal processing, signal generation, impedance readout, biosensors, nanomaterials, information visualization, machine learning.**

I. Introduction

ELECTRICAL impedance spectroscopy has been used in the characterization of materials [1] for a variety of reasons, especially because it allows for distinguishing interface from bulk phenomena [2]–[5]. It is also useful for sensing and biosensing since the electrical properties of materials are highly dependent on their interaction with the environment. Indeed, different effects can be interrogated by varying the frequency of the electrical stimulus, which is exploited in determining the interfacial changes induced in sensing experiments [6]–[9]. This has made impedance spectroscopy a method of choice for much work on sensors and biosensors [1], [10], [19], [11]–[18], particularly with sensing units comprising nanomaterials that possess large surface area-to-volume ratios [1], [20], [21]. Electrical impedance spectroscopy is based on applying an AC voltage and measuring the amplitude and phase of the response current for a range of frequencies, resulting in a complex impedance spectrum [15]. One option relies on applying a single stimulus formed by multiple frequencies, and performing a simultaneous analysis through a fast Fourier transform algorithm. However, this approach is computationally expensive, highly sensitive to noise and its complicated signal processing hardware implies big costs [22], [23]. As a result, the commercial spectrometers deal with one frequency at a time [24].

An impedance-based sensing system can be divided into three main units. The first one is the signal processing unit, responsible for the necessary conversions between the digital and the analog circuits. The second part is the sensing unit, which makes the electrical connection between the circuits and the sample, usually a liquid or gas. The data analysis unit is responsible for exploiting the digitalized impedance spectra in classification algorithms to identify the sample. In this paper we review the main concepts behind these units, with examples from the literature. Special emphasis is given to the spectrometer electronics that allow for portable and low-cost implementations. We also include a brief list of applications and challenges for using impedance spectroscopy in sensing and biosensing. This is therefore a tutorial-like article which

This work was supported in part by the São Paulo Research Foundation (FAPESP) under Grant 2018/22214-6 and Grant 2019/00101-8, and in part by the Brazilian National Council for Scientific and Technological Development (CNPq) under Grant 304312/2020.

Lorenzo A. Buscaglia and Osvaldo N. Oliveira Jr. are with the Bernhard Gross Polymers Group, Department of Physics and Materials Science, São Carlos Institute of Physics, University of São Paulo, São Carlos 13560-970, SP, Brazil (e-mails: lorenzo.buscaglia@gmail.com and chu@ifsc.usp.br).

João Paulo Carmo is with the Department of Electrical Engineering, São Carlos School of Engineering, University of São Paulo, São Carlos 13560-970, SP, Brazil (e-mail: jcarmo@sc.usp.br).

provides a roadmap for developing portable impedance spectroscopy.

II. Signal Processing

The signal processing unit receives a digital value with the frequency to be analyzed and returns the complex impedance result. This process may be split into excitation and reading. The former comprises frequency generation, involving controlled oscillation, digital-to-analog conversion and amplitude regulation. The latter regards impedance readout circuits, which involves response amplification, analog-to-digital conversion and impedance calculation.

A. Variable Frequency Signal Generation

Impedance spectroscopy requires sinusoidal signals with high harmonic quality, precise frequency, low noise and high stability against changes in the environment, especially temperature [25], [26]. Frequencies normally range between 0.1 Hz and 10 MHz and can be generated with a frequency synthesizer. This synthesizer divides the output of a fixed oscillator, or uses a variable oscillator, or even combines both. Oscillators can be classified into resistive and resonant. The former may be referred to as relaxation or non-linear oscillators; they are based on switching circuits, usually outputting a square wave, and classified as saturated and non-saturated [27], [28]. The resonant type, also known as harmonic, tuned, tank or linear oscillators, output a sinusoidal signal. In this section we discuss their application.

The best option of non-linear oscillators is known as ring oscillators and use digital circuits combined with internal and external resistors and capacitors in their implementation [27], [29]. This approach occupies less silicon area than a resonant oscillator, however it has considerably higher phase noise [30] which explains its lack of popularity in impedance spectroscopy. The resonant ones have two main types: LC and crystal oscillators. Fig. 1 (a) shows an *LC* oscillator, where $R_{loss} = Q^2 R_s$ are the ohmic losses in an inductor with quality factor Q. The conditions for this circuit to oscillate follow the Barkausen criterion [31], with a unitary closed-loop gain and a 360°-multiple phase delay. The amplifier provides a negative resistance R_{neg} allowing the circuit to oscillate at the frequency $f_{osc}=(2\pi LC)^{-1}$ when $R_{loss}>|R_{neg}|$. An *LC* oscillator generates sinusoidal waves with good degree of purity, achieving easily a Q of 60. However, it is extremely difficult to match a targeted frequency due to the L and C components industrial tolerances, which in the best case are 0.1%. A more precise way of implementing a resonant oscillator is using a crystal. This mechanical resonator transmits the signal through piezoelectric effect. Fig. 1 (b) shows the symbol and equivalent circuit of a piezoelectric crystal [32]. The electrical components in the equivalent circuit define the crystal serial resonance frequency $f_s=(2\pi L_s C_s)^{-1}$, known as Pierce oscillator. This signal frequency depends on various tunable properties of the crystal, such as shape, size and elasticity. This type of fabrication allows matching frequencies with tolerances measured in parts-per-million (ppm) and with the addition of a minimum Q of 10000 [32].

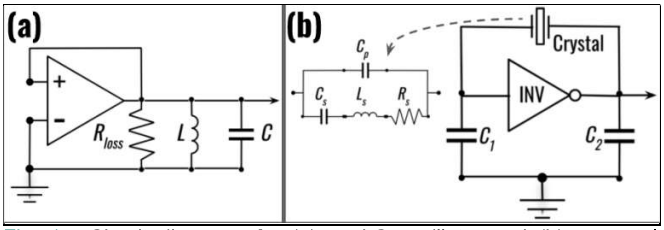

Fig. 1. Circuit diagrams for (a) an LC oscillator and (b) a crystal oscillator with the crystal's equivalent circuit.

Any of the above fixed frequency approaches can be adapted to a voltage controlled oscillator (VCO), such as the resonant *LC* ones that use variable capacitors (varactors) [33]. VCOs are used mostly in phase-locked loop (PLL) circuits with a reference frequency f_{ref}. Fig. 2 (a) shows a block diagram of a PLL, composed by a phase-frequency detector (PFD), a charge-pump (CP), a loop-filter (LF), a VCO and a frequency multiplier N, where the output frequency is $f_{out} = N f_{ref}$. LF can be freely changed by the designer to avoid the PLL's prone closed-loop instability [27], [29], [33], [34]. The LF design details, in terms of PFD and CP gain K_ϕ [2π/rad], VCO gain K_{VCO} [Hz/V] and N, can be found in reference [35]. This flexibility makes PLLs based on resonant VCOs useful for impedance spectroscopy systems, which require sine waves with high harmonic purity [36].

An alternative to generate the signal is a system known as direct digital synthesizer (DDS), also widely employed on instruments for impedance spectroscopy [15], [37]–[42]. Fig. 2 (b) shows a block diagram of a DDS comprising a reference oscillator (RO), a frequency control register (FCR), a numerically-controlled oscillator (NCO), a digital-to-analog converter (DAC) and a low-pass filter (LPF). RO establishes a maximum output frequency f_{RO}, FCR is an ordinary register based on flip-flops, and DAC is a straightforward implementation either based on R-$2R$ resistive ladders or on current source-sinks. As illustrated in Fig. 2 (b), the tricky component of DDS is NCO that consists of a phase-accumulator (PA) and a sine (and/or cosine) phase-to-amplitude converter (PAC). PAC has an internal N-bit register (PAR) which periodically accumulates the word (FCW) stored at FCR. It also contains lookup tables (LUTs) with 2^K equally-spaced values of a single oscillation cycle. Due to their symmetry, just a quarter-cycle can be used with sinusoidal waves. Usually $2^N >> 2^K$, generating a maximum truncation phase error $e \sim 360° / 2^K$. The DDS procedure starts with loading FCW into FCR to define f_{out}. In each new RO cycle, PAR accumulates FCW, resulting in $PAR_{n+1} = PAR_n + FCW$ ($PAR_0 = 0$), which gets instantly converted by DAC. Limited by the register size, when $PAR_{n+1} \geq 2^N$ it truncates, discarding the first bit and allowing the oscillation cycle to restart. The DAC output is a flat-top signal, which is then smoothed by LPF. The output frequency is given by $f_{out} = f_{RO}$ (FCW / 2^N). This fine grain to divide the f_{RO} makes DDSs more suitable for impedance spectroscopy applications than PLLs.

The DDS operation can be simulated with a microcontroller, using its memory to store the LUTs [43]. As illustrated in Fig. 2 (c), the algorithm is built with a simple structure with two adders, one multiplier block and two unit delay cells [43]. The frequency is defined by the parameter F,

between -0.2 and 0, and is given by $f_{out} = |F|^{½} (2\pi T)$, where T is the time for obtaining a single output data [43]. This approach uses sum, multiplication, analog conversion and memory access, and requires knowing the exact speed of each operation, which is usually complicated to implement.

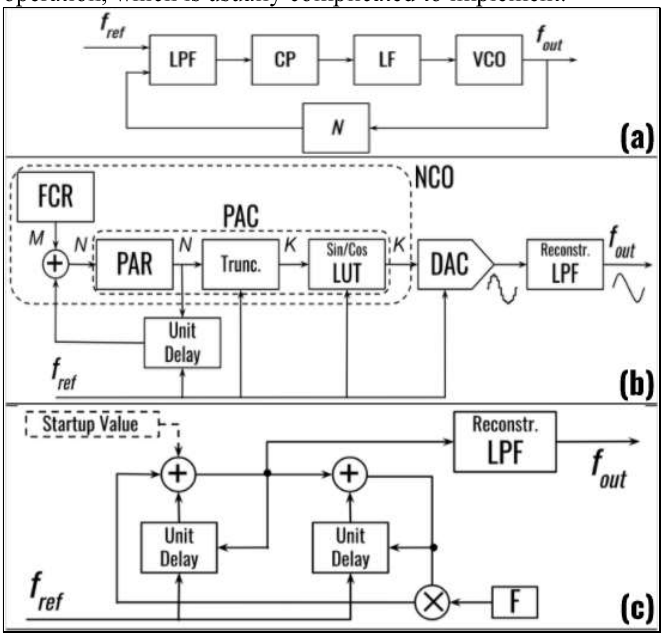

Fig. 2. Block diagrams of (a) a PLL, (b) a DDS and (c) an algorithm to simulate a DDS with a microcontroller.

B. Impedance Readout

The second part of the signal processing unit, namely the impedance readout circuit, compares the excitation and response signals and calculates the impedance, usually including an analog-to-digital converter (ADC) and a calculation core. ADCs have a limited voltage amplitude range with a limited amount of bits (resolution) and provide a maximum sampling rate. Usual impedance spectroscopy applications employ excitation amplitudes between 10 mV and 1V (2 decades) and measure impedances between 10 Ω and 10 MΩ (6 decades) [15]. This requires a highly flexible amplification strategy to fit the signal within the conversion limits without creating flattening (small amplitude) problems. Regarding the sampling rate, the frequency range usually stays within 0.1 Hz and 10 MHz (8 decades) [15], requiring hardware/software approaches capable of sweeping the full range without exceeding a reasonable duration. The recommended impedance measuring technique for frequencies up to 100 kHz is the auto-balanced bridge (ABB) [24] shown in Fig. 3 (a), based on a known feedback resistance in a current-to-voltage (I-to-V) conversion amplification. Due to the operational amplifier (op-amp) limitations, a modified ABB is suggested for frequencies from 100 kHz to 110 MHz, including null and phase detectors and a vector modulator [24]. Both settings allow calculation through comparing amplitude and phase shift before and after the I-to-V conversion. This is the main approach implemented by commercial impedance analyzers [24]. However, it has a major requirement: the sampling must be considerably faster than the signal frequency to avoid sub-sampling issues, such as aliasing and precision losses [15]. To fulfill this requirement for the highest frequencies one has to employ high-cost acquisition hardware, which hampers customized biosensing developments [44].

Most applications of electrical impedance spectroscopy in sensors and biosensors are made with frequencies below 100 kHz. This range is compatible with usual op-amps, allowing for low-cost spectrometers. Indeed, a low-cost (~ U$S 20) impedance analyzer AD5933 was made available by Analog Devices. It contains a DDS synchronized with an ADC and a 1024-point single-frequency discrete Fourier transform (DFT) multiply-accumulate (MAc) core and an I^2C communication interface [45]. This simplified hardware depicted in Fig. 3 (b) has only four options of AC amplitude, with limited impedance (>1 kΩ) and frequency (1 kHz to 100 kHz) ranges. In addition, it requires a judicious choice of amplification and calibration resistances for each application. Even with these limitations, AD5933 represented a breakthrough for low-cost impedance systems, appearing in its minimal configuration several times in the literature [46]–[49]. Some of the limitations have been surpassed with complementary peripheral circuits [50]–[56], as done in the first fully open-source device [44] and in 'Simple-Z' [57], a homemade spectrometer developed in our group. The "lock-in approach" shown in Fig. 3 (c) is an alternative for measuring impedance within the same ranges and avoiding fast sampling [58]–[61]. The response signal is analogically multiplied with sine and cosine references and passed through LPFs, outputting two DC signals representing the real (resistance) and imaginary (reactance) impedances [58]–[61]. This concept has been modified to return signals representing impedance magnitude and phase, through replacing the multipliers with modulation, comparison, XOR and integration circuits [62], as represented in Fig. 3 (d).

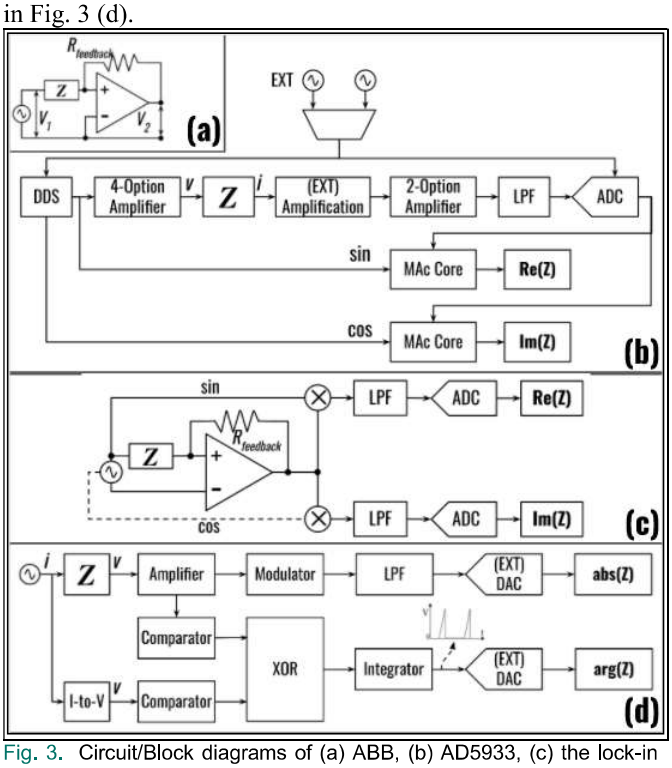

Fig. 3. Circuit/Block diagrams of (a) ABB, (b) AD5933, (c) the lock-in approach and (d) the phase/magnitude approach.

C. Instrumentation Challenges

An important issue related to signal processing is in the limitations of circuit fabrication. Analog signal processing is subjected to parasitic resistances, capacitances and inductances that alter amplitudes and phases in unwanted ways. For example, digital potentiometers such as AD5252 (Analog Devices) [63], which can be implemented as an op-amp variable feedback resistance, have significant amplitude and phase deviations for frequencies above 10 kHz [63]. Similarly, low-noise op-amps such as the AD860X (Analog Devices) series, have unideal capacitances that compromise their performance above 100 kHz [64]. Depending on the degree of impact, these problems may be addressable through software calibration. An additional issue involves the reconstruction LPF, which in some cases needs to be altered during the frequency sweep. For example, when measuring between 1 Hz and 100 kHz (5 decades), the LPF appropriate for the first decade (1-10Hz), might filter the main sinusoidal frequency if used for the last decade (10-100 kHz). The most practical solution to this problem is the selective filtering with low-noise analog multiplexing circuits (e.g. ADG7XX (Analog Devices) series) [65]. However, their parasitic capacitances have to be considered for the filtering calculations, and can even constrain the frequency range.

III. Sensing Units

Impedance spectroscopy sensors are typically fabricated through depositing electrodes over substrates and coating them with thin films of appropriate materials. These films are usually made of nanostructures, as sensitivity is enhanced when films are ultrathin. If the sensing units are biosensors, the coatings comprise a matrix onto which a bioactive layer is deposited. With molecular-specific interactions, these biosensors may be employed in clinical diagnosis and monitoring health conditions. Another extension in applications is made using an array of sensing units, rather than only a single unit. In this section we shall describe these components, including issues that might affect sensitivity and reproducibility.

A. Substrates and Electrodes

In sensing with impedance spectroscopy the electrical current goes through multiple materials and interfaces that can be represented by complex impedances [10], [15]. On one hand, serial impedances are dominated by the biggest magnitudes, motivating electrodes made from materials much more conductive than the sample [15]. Noble metals, e.g. gold [6], [20], [66]–[69], silver [70]–[72] and platinum [73], [74], or other inert metals, such as stainless steel [75], [76] and chromium [77], are normally used. On the other hand, parallel impedances are dominated by the smallest magnitudes, requiring highly insulating substrates, for example glass [67], [68], [78], silicon [69], [79]–[81], quartz [82] and alumina [78], [83]. The recent attempts to reduce costs for disposable sensing units escalated research into flexible materials, including plastics and bio-based materials such as cellulose-related substrates. Two worth highlighting areas are paper-based sensor devices [70], [84]–[87] and wearable [87]–[91] or implantable devices [92]–[94]. The latter has very stringent requirements regarding mechanical properties in addition to biocompatibility. Electrodes are fabricated via sputtering, for metal deposition, or with adsorption or printing, for inks and carbon-based materials. Screen printing and 3D printing, in particular, allow for mass production [95], [96].

The distribution of the electric field affects the detection sensitivity and depends on the electrodes geometry [18], [97], [98]. Most electrical impedance-based detections use interdigitated electrodes [7], [14], [17], [18] which may be obtained at low cost and provide good distribution within a limited area, increased signal-to-noise ratio, and can be used with small sample volumes [7]. The usual design shown in Fig. 4 (a) consists in coplanar microelectrodes with meshed parallel straight fingers forming a rectangular sensing area, fabricated by photolithography [7]. Modifying the interdigits width and interspacing can optimize sensitivity for specific applications [7], [97]. Variations of this bi-dimensional design have been explored, including wave [99], circular [100] and spiral-shaped electrodes [101], shown in Fig. 4 (b, c and d), respectively. A few three-dimensional interdigits have been explored to cover channel walls in microfluidic applications [102]. Beside interdigitated electrodes, simpler designs are used, e.g. parallel [103], [104], cylindrical [105], round [106], [107] and acicular [108] electrodes. Practically any shape can be implemented with a multi-polar sensing unit an approach that also redistributes the current paths.

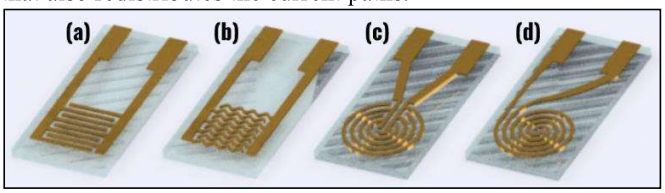

Fig. 4. Interdigitated microelectrodes design with (a) straight, (b) wavy, (c) circular and (d) spiral digits.

B. Nanomaterials for Sensors and Biosensors

The main trust in the use of nanomaterials is to increase selectivity (in the case of biosensors) and sensitivity [109], [110]. Nanomaterials can be used either in matrices or in active layers, upon exploiting the variety of molecular architectures obtained through methods allowing control in the nanoscale. The most common ones are Langmuir-Blodgett (LB) films, electrostatic layer-by-layer (LbL) films and self-assembled monolayers (SAM) [21], represented in Fig. 5 (a, b and c), respectively. The LB technique is based on transferring monolayers from insoluble molecules, organized by Van der Waals interactions at the air-water interface, onto solid supports [1]. Deposition via physical adsorption (physisorption) is possible on hydrophilic or hydrophobic substrates, through a slow vertical movement, and multilayer films can be obtained by repetition [1]. One limitation of the LB technique is in the difficulty in depositing soluble molecules, which requires special protocols [1]. This limitation was circumvented with LbL films, made from molecules in polyelectrolyte solutions deposited through electrostatic forces [1]. Furthermore, they do not require dedicated equipment, once a few beakers suffice. In contrast to these methods, SAMs are obtained with chemisorption on the substrates [111]. They are restricted to a much smaller number of possible molecules due to the chemical bonding

requirement, but are more mechanically stable [111]. The choice of the fabrication method depends on the materials employed and the principles of detection. All three techniques allow for films fabrication in a layer-by-layer fashion [112], being thus complementary to each other. They also allow immobilizing biomolecules, with their bioactivity preserved [20], and for seeking synergy in the deposition of distinct nanomaterials in the same film.

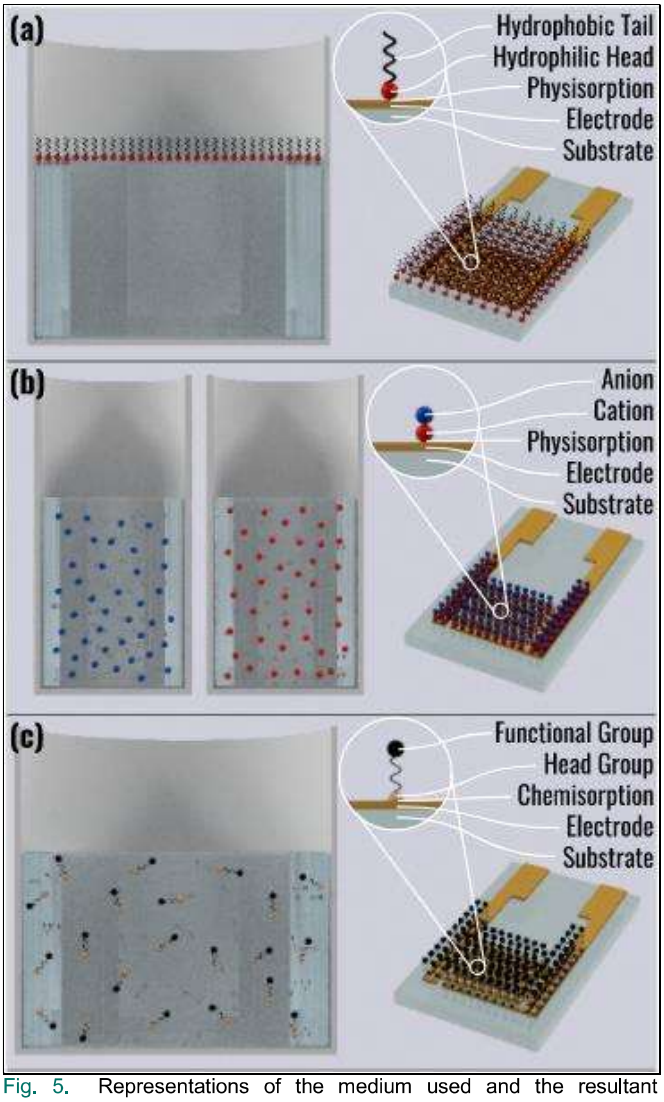

Fig. 5. Representations of the medium used and the resultant deposition of films or monolayers through the (a) LB, (b) LbL and (c) SAM techniques.

The sensing units almost always contain an ultrathin film coating the electrodes. As already mentioned most these coatings involve nanomaterials, as discussed at length in reference [112]. Carbon-based materials such as carbon nanotubes and graphene have been prominent in sensors and biosensors, where in the latter they usually comprise the matrix for the immobilization of biomolecules [112]. Also worth mentioning are the metallic nanoparticles, especially silver and gold, as they affect the electrical properties of the sensing units, which may be exploited in increasing the sensitivity [112]. Similarly to the carbon-based materials, nanoparticles can be incorporated in the matrix of biosensors [112]. The synergy sought in combining nanomaterials and biomolecules is perhaps the most important feature in developing biosensors at present. The extensive use of biosensing has motivated the establishing new nomenclatures in the topic. It is often the case that biosensors are referred to by their classes. Then, biosensors can be called enzymatic biosensors, immunosensors when the antigen-antibody interaction is explored, and genosensors for detecting genetic material (DNA or RNA) [112]. DNA-based sensing is expected to change the landscape of clinical diagnosis, as it can replace expensive procedures such as polymerase chain reaction (PCR) that requires sophisticated equipment [9], [113]. An example of a genosensor is the highly specific detection of a DNA sequence of SARS-CoV-2, which was performed with a portable impedance analyzer [57]. The most popular biosensors, available in commercial products, are made with enzymes. The immobilization process of the enzymes is performed with various techniques, for example with LbL films for detecting catechol [114].

C. Arrays of Sensing Units

Impedance spectroscopy is also useful in sensing tasks where an array of sensing units is employed, rather than a single unit. Two main cases require such arrays: (i) monitoring/detecting multiple analytes, using distinct sensors/biosensors, and (ii) mapping impedance spatial distribution, using identical units. An example of the former case is an electronic tongue for taste detection in liquid samples, represented in Fig. 6 (a), where multiple sensing units of different materials provide a matrix of information for global selectivity [75]. The latter case is represented by tomographies, as in Fig. 6 (b and c), where the bi or tri-dimensional location of each tissue is sought [115], [116]. In these applications identical electrodes strategically distributed in a spatial matrix. The impedance results through this matrix are combined to produce the desired image [10], [116], [117]. Similar approaches are used for measuring position, growth and movement [118]–[121]. In most uses of the arrays mentioned numerous measurements have to be performed, which can be done simultaneously with very high-speed sampling circuits, using sample-and-hold techniques [15], [122], or with parallel-acquisition circuits [123]. However, these simultaneous sampling approaches result in expensive systems. Low-cost alternatives reside in sequential measurements, automatically performed with programmable switching circuits. Relays are useful for laboratory settings [124], but their high dimensions, weight and power consumption hinder portable applications. Smaller CMOS analog multiplexers, e.g. the ADG7XX series [65], are suitable for portable and wearable systems. Indeed, in recent years pixel-like matrices of sensing units were incorporated into the CMOS circuits [73], [119], [125], [126]. This approach allows for a very large number of electrodes, useful for example for cells counting, as shown in Fig. 6 (d) [125].

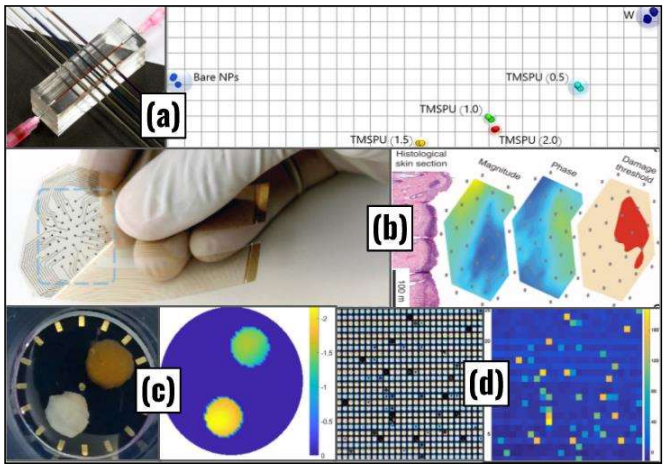

Fig. 6. Arrays of sensing units and visualization techniques for (a) an electronic tongue [75], (b and c) bi-dimensional tomographies [115], [116] and (d) pixel-based cell counting [125].

D. Common Interferences

In highly-sensitive detection techniques, slight systematic errors can compromise the results. In sensing with electrical impedance spectroscopy there are two main issues to consider: electrode polarization and tracks exposure. Polarization is relevant in electrolytic solutions where the electrodes surface tend to get covered with a layer of ions, of opposite charges, forming an electrical double layer [15]. This phenomenon, represented in Fig. 7 (a), produces a capacitive electrical barrier, often modeled as capacitance in series with the sample [15]. The impedance of the double layer is higher at low frequencies. When it is much higher than the sample impedance, the sensitivity is compromised [127]. The establishment of the double layer may take some minutes [128], and this needs to be considered in measurement protocols. The polarization impedance depends on the electrodes material, with platinum being advantageous, especially if platinum black is used, which can reduce polarization impedance by up to four orders of magnitude [128]. Since varying the electrodes geometry can also reduce polarization [129], interdigitated nanoelectrodes with dimensions near the Debye length (hundreds of nm) have been explored to enhance sensitivity [130], [131]. As for the interference regarding the connection tracks in contact with the liquid sample, it results in a parallel capacitance in the impedance model that also affects the detection performance [132], [133]. The tracks width has a direct relation to the normalized impedance variation [133]. Aiming for a reproducible measurement, several articles include an insulation layer (usually PDMS) that works as a chamber for the liquid sample [83], [134], [135], as shown in Fig. 7 (b). This also avoids variations in the drop interfacial area [83], [135].

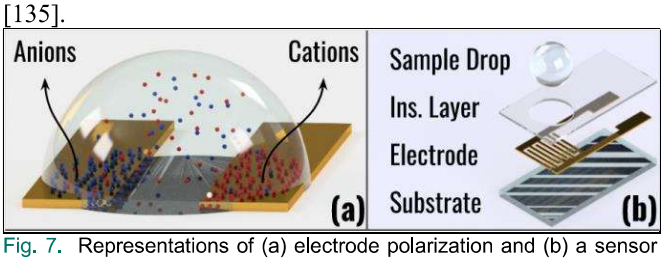

Fig. 7. Representations of (a) electrode polarization and (b) a sensor with an insulation layer.

IV. Biosensing and other Applications

The number of papers published involving the use of impedance spectroscopy for sensing and biosensing has increased steadily of the last decade. A brief survey in scientific databases retrieves more than 10,000 papers, which also include electrochemical impedance spectroscopy – not considered in this review paper. Most of this work was produced since 2000, as the number of papers per year in the early 1990s was just a few. Review papers have covered considerable parts of this work, normally with focus on applications. For example, impedance-based electronic tongues have been reviewed in reference [136]. In recent years we note an increasing emphasis in biosensors, especially with low-cost systems that are being developed toward point-of-care diagnosis. Because of this trend we present below just a summary account of impedance spectroscopy for biosensing.

Nearly all articles in this topic can be classified into three groups: clinical diagnosis, food quality control and cell cultures monitoring. The first group is dominated by the detection of viruses and microorganisms, such as those for Avian Influenza [137], Hepatitis B [138], HPV16 [139] , Covid-19 [57], E. Coli [70], [140]–[142], S. Aureus [110], [143], [144], S. Epidermidis [145], M. Tuberculosis [72], Salmonella Typhi [146] and Brettanomyces [147]. Research into early cancer diagnosis is right behind, including breast [21], [69], [103], prostate [9], [148], pancreas [20], [149]–[151], colon [152] and thyroid cancers [153]. Body composition bioimpedance analysis (BIA) [154] and impedance cardiography (ICG) [13] are also noteworthy, since they constitute the most commercially explored applications. Other health-related biomarkers such as cholesterol [155], cortisol [104], pH [87], glucose and triglycerides [156], have also been detected with impedance spectroscopy. Now regarding the second group, food quality involves the analysis of taste and composition, especially for contamination or adulteration. Electronic tasting has been proved useful for wines [157], honey [158], mineral water [159], ice-cream [76]. and fruits [160]. Contamination can occur with bacteria, detected as for clinical diagnosis, or with toxic pesticides, detectable through electronic tasting [161]. The last group of articles also involves cell cultures, such as bacteria or tumors, however with focus on low-cost and fast alternatives for monitoring quantity and position, usually with arrays [120], [162].

V. Data Analysis and Classification

The trend toward ubiquitous sensing and biosensing, in surveillance, monitoring and diagnosis systems, has led to an enormous amount of data, whose processing requires computational and statistical tools. In order to deal with such data, it is useful to recall that from a conceptual - or semantic - perspective, sensing or biosensing corresponds to a classification task. This definition is relevant because of the large body of knowledge accumulated over the years to classify objects or processes, mostly by research communities in statistics and computer science [12], [163], [164]. Data from sensors and biosensors have long been treated with

statistical methods belonging to the realms of chemometrics [165]. There are some applications in which the necessary classification can be done by measuring impedance at a single frequency, chosen from the spectra to optimize the detection sensitivity. In these cases, a calibration curve relating the impedance to the sought property is used [20], [69], [166], [167]. When this is possible, it naturally allows for implementations based on very low-cost single-frequency hardware. However, disregarding the rest of the spectrum means that the potential of classification is diminished, especially as far as selectivity is concerned. In recent years sensing and biosensing data analysis has been extended with the use of information visualization (InfoViz) methods [19], [168]. These embrace linear techniques, such as principal component analysis (PCA) [19], [161], [168], [169], and non-linear ones, such as Sammon's mapping [19], [144], [166], [168], [170], interactive document mapping (IDMAP) [19], [109], [110], [144], [168], [170], [171] and parallel coordinates [19], [110], [112], [168]. It is noteworthy that the non-linear technique IDMAP, exemplified in Fig. 6 (a), was conceived to classify texts and turned out the most efficient one for biosensing data analysis, enhancing the capability of discriminating complex samples. Perhaps the most relevant advantage of InfoViz is the ability to process a whole dataset rather than portions of it, as normally done in manual analysis. Furthermore, it is possible to perform feature selection by assessing the discrimination ability of the sensing units with metrics such as the silhouette coefficient [9], [19], [110], [148], [168].

Data analysis with these multidimensional projections can be complemented with unsupervised and supervised machine learning (ML) [172]. Both have been proven effective in classification tasks, in spite of its limitations in addressing problems requiring interpretation. Therefore, the trend toward ML to analyze sensing and biosensing data seems irreversible (see for instance some discussion in other review papers [12], [163], [164], [173]). The effectiveness of ML methods depends on the amount of data and its coverage of the universe under analysis. In such approaches, different types of data may be integrated to improve classification, especially for clinical diagnostics as the ones cited in section IV. Besides impedance spectroscopy scientific data, text and images can also be employed [109]. To our knowledge, the first use of ML for impedance spectroscopy data was for correlating electronic tongue results with human taste for Brazilian coffee samples [174]. Since then, several articles explored this approach [175]–[177], and the new concept of multidimensional calibration space based on machine learning is likely to further boost such applications [doi:10.1246/bcsj.2020-0359].

VI. Conclusions and Future Perspectives

In this survey we have described the basic concepts, latest developments and instrumentation issues of the different parts of an electrical impedance spectroscopy system, which have mostly been considered separately in the literature. The major emphasis was given to the signal processing circuitry in order to cover the significant progress in recent years. This progress is making it possible to overcome bottlenecks that prevented the implementation of portable devices. More specifically, we introduced a kind of roadmap for implementing low-cost portable impedance spectroscopy devices, much cheaper than the available commercial impedance analyzers (> 1k USD). The reduction in price may now enable a global and massive use of impedance spectroscopy in higher education laboratories, in addition to its application for point-of-care clinical diagnosis, food quality control and cell culture monitoring. Also discussed in the paper were the data analysis methods, including information visualization and machine learning, which will be essential to deal with the large amounts of data to be generated in these envisaged applications.

References

[1] J. R. Siqueira, L. Caseli, F. N. Crespilho, V. Zucolotto, and O. N. Oliveira, "Immobilization of biomolecules on nanostructured films for biosensing," *Biosens. Bioelectron.*, vol. 25, pp. 1254–1263, Oct. 2010, doi: 10.1016/j.bios.2009.09.043.

[2] J. C. Valer, G. Roberts, A. Chambers, J. Owen, and M. Roberts, "Using Zinc Oxide Thick Films," *IEEE Sens. J.*, vol. 13, no. 8, pp. 3046–3052, Aug. 2013, doi: 10.1109/JSEN.2013.2257730.

[3] D. Polese *et al.*, "AC characterization of nitrate intercalated layered double hydroxides gas sensors," in *2017 IEEE Sensors*, Dec. 2017, pp. 1–3, doi: 10.1109/ICSENS.2017.8234323.

[4] M. Nasir, D. T. Price, L. C. Shriver-Lake, and F. Ligler, "Effect of diffusion on impedance measurements in a hydrodynamic flow focusing sensor," *Lab Chip*, vol. 10, pp. 2787–2795, Aug. 2010, doi: 10.1039/c005257d.

[5] K. Aguir, A. Labidi, and C. Lambert-Mauriat, "Impedance spectroscopy to identify the conduction mechanisms in WO3 sensors," in *IEEE Sensors 2006*, Oct. 2006, pp. 267–270, doi: 10.1109/ICSENS.2007.355771.

[6] N. Hasan, W. Zhang, and A. D. Radadia, "Characterization of Nanodiamond Seeded Interdigitated Electrodes using Impedance Spectroscopy of Pure Water," *Electrochim. Acta*, vol. 210, pp. 375–382, May 2016, doi: 10.1016/j.electacta.2016.05.053.

[7] X. F. Yan, M. H. Wang, and D. An, "Progress of interdigitated array microelectrodes based impedance immunosensor," *Chinese J. Anal. Chem.*, vol. 39, no. 10, pp. 1601–1610, Mar. 2011, doi: 10.1016/S1872-2040(10)60478-1.

[8] B. A. Mazzeo and A. J. Flewitt, "Observation of protein-protein interaction by dielectric relaxation spectroscopy of protein solutions for biosensor application," *Appl. Phys. Lett.*, vol. 90, no. 123901, pp. 1–3, Mar. 2007, doi: 10.1063/1.2716350.

[9] J. C. Soares *et al.*, "Detection of the Prostate Cancer Biomarker PCA3 with Electrochemical and Impedance-Based Biosensors," *ACS Appl. Mater. Interfaces*, vol. 11, pp. 46645–46650, Nov. 2019, doi: 10.1021/acsami.9b19180.

[10] M. R. Baidillah, A. A. S. Iman, Y. Sun, and M. Takei, "Electrical Impedance Spectro-Tomography Based on Dielectric Relaxation Model," *IEEE Sens. J.*, vol. 17, no. 24, pp. 8251–8262, Dec. 2017, doi: 10.1109/JSEN.2017.2710146.

[11] E. Katz and I. Willner, "Probing biomolecular interactions at conductive and semiconductive surfaces by impedance spectroscopy: Routes to impedimetric immunosensors, DNA-sensors, and enzyme biosensors," *Electroanalysis*, vol. 15, no. 11, pp. 913–947, Feb. 2003, doi: 10.1002/elan.200390114.

[12] H. Caytak, A. Boyle, A. Adler, and M. Bolic, "Bioimpedance Spectroscopy Processing and Applications," *Encycl. Biomed. Eng.*, vol. 3, pp. 265–279, 2019, doi: 10.1016/B978-0-12-801238-3.10884-0.

[13] J. C. Miller and S. M. Horvath, "Impedance Cardiography," *Psychophysiology*, vol. 15, no. 1, pp. 80–91, 1978, doi: 10.1111/j.1469-8986.1978.tb01340.x.

[14] H. Jiang, M. Zhang, B. Bhandari, and B. Adhikari, "Application of electronic tongue for fresh foods quality evaluation: A review," *Food Rev. Int.*, vol. 34, no. 8, pp. 746–769, Jan. 2018, doi: 10.1080/87559129.2018.1424184.

[15] L. Callegaro, *Electrical Impedance: Principles, Measurement and Applications*. New York, USA: CRC Press, 2013.

[16] M. L. Moraes *et al.*, "Strategies to optimize biosensors based on

impedance spectroscopy to detect phytic acid using layer-by-layer films," *Anal. Chem.*, vol. 82, no. 8, pp. 3239–3246, Apr. 2010, doi: 10.1021/ac902949h.

[17] J. Huang, Y. Zhang, and J. Wu, "Review of non-invasive continuous glucose monitoring based on impedance spectroscopy," *Sensors Actuators A Phys.*, vol. 311, no. 112103, pp. 1–9, May 2020, doi: 10.1016/j.sna.2020.112103.

[18] Y. Xu, X. Xie, Y. Duan, L. Wang, Z. Cheng, and J. Cheng, "A review of impedance measurements of whole cells," *Biosens. Bioelectron.*, vol. 77, pp. 824–836, Oct. 2016, doi: 10.1016/j.bios.2015.10.027.

[19] F. V. Paulovich, M. L. Moraes, R. M. Maki, M. Ferreira, O. N. Oliveira Jr., and M. C. F. de Oliveira, "Information visualization techniques for sensing and biosensing," *Analyst*, vol. 136, no. 7, p. 1344, Apr. 2011, doi: 10.1039/c0an00822b.

[20] A. Thapa *et al.*, "Carbon Nanotube Matrix for Highly Sensitive Biosensors to Detect Pancreatic Cancer Biomarker CA19-9," *ACS Appl. Mater. Interfaces*, vol. 9, no. 31, pp. 25878–25886, Jul. 2017, doi: 10.1021/acsami.7b07384.

[21] J. C. Soares, F. M. Shimizu, A. C. Soares, L. Caseli, J. Ferreira, and O. N. Oliveira, "Supramolecular Control in Nanostructured Film Architectures for Detecting Breast Cancer," *ACS Appl. Mater. Interfaces*, vol. 7, no. 22, pp. 11833–11841, May 2015, doi: 10.1021/acsami.5b03761.

[22] X. Liu, L. Li, and A. J. Mason, "High-Throughput impedance spectroscopy biosensor array chip," *Philos. Trans. R. Soc. A Math. Phys. Eng. Sci.*, vol. 372, no. 2012, pp. 1–14, Mar. 2014, doi: 10.1098/rsta.2013.0107.

[23] A. Sanchez-Gonzalez, N. Medrano, B. Calvo, and P. A. Martinez, "A multichannel FRA-based impedance spectrometry analyzer based on a low-cost multicore microcontroller," *Electron.*, vol. 8, no. 38, pp. 1–23, Jan. 2019, doi: 10.3390/electronics8010038.

[24] *Impedance Measurement Handbook: A guide to measurement technology and techniques*, 4th Editio. Agilent Technologies, 2009.

[25] Y. Wang, P. K. Chan, and K. H. Li, "A compact CMOS ring oscillator with temperature and supply compensation for sensor applications," in *Proceedings of IEEE Computer Society Annual Symposium on VLSI*, Jul. 2014, pp. 267–272, doi: 10.1109/ISVLSI.2014.15.

[26] E. Lindberg, "Oscillators - A simple introduction," in *European Conference on Circuit Theory and Design Proceedings*, 2013, no. 1912, pp. 1–4.

[27] J. P. Carmo, P. M. Mendes, and J. H. Correia, "A 4.2 mW 5.7-GHz frequency synthesizer with dynamic-logic (TSPC) frequency divider," in *16th International Conference on Telecommunications*, May 2009, pp. 309–312, doi: 10.1109/ICTEL.2009.5158664.

[28] Chan-Hong Park and Beomsup Kim, "A low-noise 900 MHz VCO in 0.6 μm CMOS," *IEEE J. Solid-State Circuits*, vol. 34, no. 5, pp. 586–591, May 1999, doi: 10.1109/vlsic.1998.687991.

[29] J. P. Carmo and J. H. Correia, "RF CMOS transceiver at 2.4 GHz in wearables for measuring the cardio-respiratory function," *Measurement*, vol. 44, no. 1, pp. 65–73, Jan. 2011, doi: 10.1016/j.measurement.2010.09.027.

[30] T. H. Lee and A. Hajimiri, "Oscillator phase noise: A tutorial," *IEEE J. Solid-State Circuits*, vol. 35, no. 3, pp. 326–335, Mar. 2000, doi: 10.1109/4.826814.

[31] Y. K. Rybin, "Barkhausen criterion for pulse oscillators," *Int. J. Electron.*, vol. 99, no. 11, pp. 1547–1556, Apr. 2012, doi: 10.1080/00207217.2012.673153.

[32] R. G. Meyer and D. C. F. Soo, "MOS Crystal Oscillator Design," *IEEE J. Solid-State Circuits*, vol. SC-15, no. 2, pp. 222–228, Apr. 1980, doi: 10.1109/JSSC.1980.1051366.

[33] S. Pellerano, S. Levantino, C. Samori, and A. L. Lacaita, "A 13.5-mW 5-GHz Frequency Synthesizer with Dynamic-Logic Frequency Divider," *IEEE J. Solid-State Circuits*, vol. 39, no. 2, pp. 378–383, Feb. 2004, doi: 10.1109/JSSC.2003.821784.

[34] F. M. Gardner, "Charge-pump phase-lock loops," *Monolith. Phase-Locked Loops Clock Recover. Circuits Theory Des.*, vol. COM-28, no. 11, pp. 1849–1858, Nov. 1980, doi: 10.1109/9780470545331.ch4.

[35] J. P. Carmo, P. M. Mendes, C. Couto, and J. H. Correia, "A 3.4-mW 2.4-GHz frequency synthesizer in 0.18 um CMOS," in *4th International Conference on Design & Technology of Integrated Systems in Nanoscal Era*, Apr. 2009, pp. 266–269, doi: 10.1109/DTIS.2009.4938068.

[36] J. Kim, M. A. Abbasi, T. Kim, K. D. Park, and S. Cho, "Lock-in amplifier-based impedance detection of tissue type using a monopolar injection needle," *Sensors*, vol. 19, no. 21, pp. 1–9, Oct. 2019, doi: 10.3390/s19214614.

[37] A. Al-Ali, A. Elwakil, A. Ahmad, and B. Maundy, "Design of a portable low-cost impedance analyzer," in *10th International Conference on Biomedical Electronics and Devices*, Feb. 2017, vol. 1, pp. 104–109, doi: 10.5220/0006121901040109.

[38] M. Carminati, G. Ferrari, D. Bianchi, and M. Sampietro, *Impedance Spectroscopy for Biosensing: Circuits and Applications*. New York, USA: Springer, 2015.

[39] H. Dastjerdi, R. Soltanzadeh, and H. Rabbani, "Designing and Implementing Bioimpedance Spectroscopy Device by Measuring Impedance in a Mouse Tissue," *J. Med. Signals Sens.*, vol. 3, no. 3, pp. 187–194, Jul. 2013, doi: 10.4103/2228-7477.120979.

[40] A. A. A. Al-Ali, "Design and Implementation of a Magnitude Only Bio-Impedance Analyzer," University of Calgary, Calgary, Canada, 2018.

[41] S. Sherif, O. E. Morsy, L. Ziko, R. Siam, Y. H. Ghallab, and Y. Ismail, "Integration of tri-polar microelectrodes for performance enhancement of an impedance biosensor," *Sens. Bio-Sensing Res.*, vol. 28, no. 100329, pp. 1–13, Jun. 2020, doi: 10.1016/j.sbsr.2020.100329.

[42] M. Flatscher, M. Neumayer, T. Bretterklieber, and B. Schweighofer, "Measurement of Complex Dielectric Material Properties of Ice using Electrical Impedance Spectroscopy," in *IEEE Sensors*, Oct. 2016, pp. 1–3, doi: 10.1109/ICSENS.2016.7808533.

[43] D. Danieli, "Microcontroller provides an alternative to DDS," *EDN*, Jan. 2010. .

[44] D. M. Jenkins, B. E. Lee, S. Jun, J. Reyes-De-Corcuera, and E. S. McLamore, "ABE-Stat, a Fully Open-Source and Versatile Wireless Potentiostat Project Including Electrochemical Impedance Spectroscopy," *J. Electrochem. Soc.*, vol. 166, no. 9, pp. B3056–B3065, Mar. 2019, doi: 10.1149/2.0061909jes.

[45] *AD5933 Datasheet*. Norwood, USA: Analog Devices, 2005.

[46] A. Pal, D. Goswami, H. E. Cuellar, B. Castro, S. Kuang, and R. V. Martinez, "Early detection and monitoring of chronic wounds using low-cost, omniphobic paper-based smart bandages," *Biosens. Bioelectron.*, vol. 117, pp. 696–705, Oct. 2018, doi: 10.1016/j.bios.2018.06.060.

[47] M. Vishnu Chittan, M. K. Chimpineni, B. Rajesh Kumar, and D. Sailaja, "Design and Development of Cost-Effective System for the Measurement of Dielectric Constant of Ceramic Materials Using PIC Microcontroller," *MAPAN - J. Metrol. Soc. India*, vol. 34, no. 4, pp. 443–450, Dec. 2019, doi: 10.1007/s12647-019-00313-z.

[48] G. Naishadham, E. Bekyarova, Y. Qian, and K. Naishadham, "Design of Low-Frequency Impedance Measurement Sensors for Respiratory Health," in *IEEE Sensors*, Oct. 2018, pp. 1–4, doi: 10.1109/ICSENS.2018.8589787.

[49] C. J. Chen, J. T. Liu, S. J. Chang, M. W. Lee, and J. Z. Tsai, "Development of a portable impedance detection system for monitoring the growth of mouse L929 cells," *J. Taiwan Inst. Chem. Eng.*, vol. 43, no. 5, pp. 678–684, May 2012, doi: 10.1016/j.jtice.2012.04.008.

[50] M. Hefele, W. Wirths, M. Brischwein, H. Grothe, F. Kreupl, and B. Wolf, "Measuring fluorescence-lifetime and bio-impedance sensors for cell based assays using a network analyzer integrated circuit," *Biosens. Bioelectron.*, vol. 129, pp. 292–297, Sep. 2019, doi: 10.1016/j.bios.2018.09.053.

[51] A. Hafid, S. Benouar, M. Kedir-Talha, F. Abtahi, M. Attari, and F. Seoane, "Full Impedance Cardiography Measurement Device Using Raspberry PI3 and System-on-Chip Biomedical Instrumentation Solutions," *IEEE J. Biomed. Heal. Informatics*, vol. 22, no. 6, pp. 1883–1894, Nov. 2018, doi: 10.1109/JBHI.2017.2783949.

[52] C. Margo, J. Katrib, M. Nadi, and A. Rouane, "A four-electrode low frequency impedance spectroscopy measurement system using the AD5933 measurement chip," *Physiol. Meas.*, vol. 34, no. 4, pp. 391–405, Mar. 2013, doi: 10.1088/0967-3334/34/4/391.

[53] A. V. Shlyakhotka, E. K. Lyakhova, and A. D. Sutyagina, "Design of a device for determining stroke volume by the impedance cardiography method," in *IEEE Conference of Russian Young Researchers in Electrical and Electronic Engineering*, Jan. 2018, pp. 1225–1226, doi: 10.1109/EIConRus.2018.8317313.

[54] R. Harder, A. Diedrich, J. S. Whitfield, M. S. Buchowski, J. B. Pietsch, and F. J. Baudenbacher, "Smart Multi-Frequency

Bioelectrical Impedance Spectrometer for BIA and BIVA Applications," *IEEE Trans. Biomed. Circuits Syst.*, vol. 10, no. 4, pp. 912–919, Aug. 2016, doi: 10.1109/TBCAS.2015.2502538.

[55] B. Van Grinsven *et al.*, "Customized impedance spectroscopy device as possible sensor platform for biosensor applications," *Phys. Status Solidi A Appl. Mater. Sci.*, vol. 207, no. 4, pp. 919–923, Mar. 2010, doi: 10.1002/pssa.200983305.

[56] K. Chabowski, T. Piasecki, A. Dzierka, and K. Nitsch, "SIMPLE WIDE FREQUENCY RANGE IMPEDANCE METER BASED ON AD5933 INTEGRATED CIRCUIT," *Metrol. Meas. Syst.*, vol. XXII, no. 1, pp. 13–24, Mar. 2015, doi: 10.1515/mms-2015-0006.K.

[57] J. C. Soares *et al.*, "Detection of a SARS-CoV-2 Sequence with Genosensors Using Data Analysis Based on Information Visualization and Machine Learning Techniques," *ChemRxiv - Unpubl. Artic.*, 2020, doi: 10.26434/chemrxiv.13366379.v1.

[58] A. Hedayatipour, S. Aslanzadeh, and N. McFarlane, "CMOS based whole cell impedance sensing: Challenges and future outlook," *Biosens. Bioelectron.*, vol. 143, no. 111600, pp. 1–13, Aug. 2019, doi: 10.1016/j.bios.2019.111600.

[59] H. Jafari, L. Soleymani, and R. Genov, "16-channel CMOS impedance spectroscopy DNA analyzer with dual-slope multiplying ADCs," *IEEE Trans. Biomed. Circuits Syst.*, vol. 6, no. 5, pp. 468–478, Oct. 2012, doi: 10.1109/TBCAS.2012.2226334.

[60] A. Manickam, A. Chevalier, M. McDermott, A. D. Ellington, and A. Hassibi, "A CMOS Electrochemical Impedance Spectroscopy (EIS) Biosensor Array," *IEEE Trans. Biomed. Circuits Syst.*, vol. 4, no. 6, pp. 379–390, Dec. 2010, doi: 10.1109/TBCAS.2010.2081669.

[61] A. Rottigni, M. Carminati, G. Ferrari, and M. Sampietro, "Handheld Bio-Impedance Measurement System Based on an Instrument-on-Chip," in *7th Conference on Ph.D. Research in Microelectronics and Electronics*, Jul. 2011, pp. 49–52, doi: 10.1109/PRIME.2011.5966214.

[62] P. Kassanos, I. F. Triantis, and A. Demosthenous, "A CMOS magnitude/phase measurement chip for impedance spectroscopy," *IEEE Sens. J.*, vol. 13, no. 6, pp. 2229–2236, Jun. 2013, doi: 10.1109/JSEN.2013.2251628.

[63] *AD5251/AD5252 Datasheet*. Norwood, USA: Analog Devices, 2004.

[64] *AD8605/AD8606/AD8608 Datasheet*. Norwood, USA: Analog Devices, 2002.

[65] *ADG728/ADG729 Datasheet*. Norwood, USA: Analog Devices, 2012.

[66] M. F. P. da Silva *et al.*, "Synthesis and characterization of GO-H3BO3 composite for improving single-sensor impedimetric olfaction," *J. Mater. Sci. Mater. Electron.*, vol. 31, no. 17, pp. 14443–14453, Jul. 2020, doi: 10.1007/s10854-020-04004-3.

[67] Z. B. Jildeh, J. Oberländer, P. Kirchner, M. Keusgen, P. H. Wagner, and M. J. Schöning, "Experimental and Numerical Analyzes of a Sensor Based on Interdigitated Electrodes for Studying Microbiological Alterations," *Phys. Status Solidi A Appl. Mater. Sci.*, vol. 215, no. 15, pp. 1–9, May 2018, doi: 10.1002/pssa.201700920.

[68] C. M. Daikuzono *et al.*, "Information Visualization and Feature Selection Methods Applied to Detect Gliadin in Gluten-Containing Foodstuff with a Microfluidic Electronic Tongue," *ACS Appl. Mater. Interfaces*, vol. 9, no. 23, pp. 19646–19652, May 2017, doi: 10.1021/acsami.7b04252.

[69] R. Gajasinghe, M. Jones, T. A. Ince, and O. Tigli, "Label and Immobilization Free Detection and Differentiation of Tumor Cells," *IEEE Sens. J.*, vol. 18, no. 9, pp. 3486–3493, May 2018, doi: 10.1109/JSEN.2018.2813975.

[70] D. Mondal, R. Binish, S. Samanta, D. Paul, and S. Mukherji, "Detection of Total Bacterial Load in Water Samples Using a Disposable Impedimetric Sensor," *IEEE Sens. J.*, vol. 20, no. 4, pp. 1712–1720, Feb. 2020, doi: 10.1109/JSEN.2019.2950422.

[71] P. Mostafalu and S. Sonkusale, "A high-density nanowire electrode on paper for biomedical applications," *RSC Adv.*, vol. 5, no. 12, pp. 8680–8687, Jan. 2015, doi: 10.1039/c4ra12373e.

[72] S. C. B. Gopinath *et al.*, "Nanogapped impedimetric immunosensor for the detection of 16 kDa heat shock protein against Mycobacterium tuberculosis," *Microchim. Acta*, vol. 183, no. 10, pp. 2697–2703, Jul. 2016, doi: 10.1007/s00604-016-1911-7.

[73] V. Vijay *et al.*, "High-density CMOS Microelectrode Array System for Impedance Spectroscopy and Imaging of Biological Cells," in *IEEE Sensors*, Oct. 2016, pp. 1–3, doi: 10.1109/TBCAS.2018.2881044.

[74] A. Tura, S. Sbrignadello, S. Barison, S. Conti, and G. Pacini, "Impedance spectroscopy of solutions at physiological glucose concentrations," *Biophys. Chem.*, vol. 129, pp. 235–241, Jun. 2007, doi: 10.1016/j.bpc.2007.06.001.

[75] F. M. Shimizu *et al.*, "Monitoring the Surface Chemistry of Functionalized Nanomaterials with a Microfluidic Electronic Tongue," *ACS Sensors*, vol. 3, no. 3, pp. 716–726, Feb. 2018, doi: 10.1021/acssensors.8b00056.

[76] M. Grossi, M. Lanzoni, R. Lazzarini, and B. Riccò, "Automatic ice-cream characterization by impedance measurements for optimal machine setting," *Measurement*, vol. 45, no. 7, pp. 1747–1754, Apr. 2012, doi: 10.1016/j.measurement.2012.04.009.

[77] C. E. Borato *et al.*, "Layer-by-layer Films of Poly(o-ethoxyaniline), Chitosan and Chitosan-poly(methacrylic acid) Nanoparticles and their Application in an Electronic Tongue," *IEEE Trans. Dielectr. Electr. Insul.*, vol. 13, no. 5, pp. 1101–1109, Oct. 2006, doi: 10.1109/TDEI.2006.247838.

[78] A. R. M. Syaifudin *et al.*, "Measurements and Performance Evaluation of Novel Interdigital Sensors for Different Chemicals Related to Food Poisoning," *IEEE Sens. J.*, vol. 11, no. 11, pp. 2957–2965, Nov. 2011, doi: 10.1109/JSEN.2011.2154327.

[79] S. MacKay, G. N. Abdelrasoul, M. Tamura, D. Lin, Z. Yan, and J. Chen, "Using impedance measurements to characterize surface modified with gold nanoparticles," *Sensors*, vol. 17, no. 2141, pp. 1–16, Sep. 2017, doi: 10.3390/s17092141.

[80] K. L. Foo, U. Hashim, C. H. Voon, M. Kashif, and M. E. Ali, "Au decorated ZnO thin film: application to DNA sensing," *Microsyst. Technol.*, vol. 22, no. 4, pp. 903–910, May 2016, doi: 10.1007/s00542-015-2572-x.

[81] S. K. Srivastava *et al.*, "A generic microfluidic biosensor of G protein-coupled receptor activation - impedance measurements of reversible morphological changes of reverse transfected HEK293 cells on microelectrodes," *RSC Adv.*, vol. 5, no. 65, pp. 52563–52570, Jun. 2015, doi: 10.1039/c5ra04976h.

[82] E. R. Carvalho, N. C. Filho, E. C. Venancio, N. O. Osvaldo, L. H. C. Mattoso, and L. Martin-Neto, "Detection of brominated by-products using a sensor array based on nanostructured thin films of conducting polymers," *Sensors*, vol. 7, no. 12, pp. 3258–3271, Dec. 2007, doi: 10.3390/s7123258.

[83] X. Zheng *et al.*, "Generic protease detection technology for monitoring periodontal disease," *Faraday Discuss.*, vol. 149, pp. 37–47, Oct. 2011, doi: 10.1039/c005364c.

[84] R. M. Morais, M. D. S. Klem, G. L. Nogueira, T. C. Gomes, and N. Alves, "Low Cost Humidity Sensor Based on PANI/PEDOT:PSS Printed on Paper," *IEEE Sens. J.*, vol. 18, no. 7, pp. 2647–2651, Apr. 2018, doi: 10.1109/JSEN.2018.2803018.

[85] C. M. Daikuzono, C. Delaney, A. Morrin, D. Diamond, L. Florea, and O. N. Oliveira, "Paper based electronic tongue-a low-cost solution for the distinction of sugar type and apple juice brand," *Analyst*, vol. 144, no. 8, pp. 2827–2832, Mar. 2019, doi: 10.1039/c8an01934g.

[86] D. Mondal, D. Paul, and S. Mukherji, "Impedance Spectroscopy-Based Detection of Cardiac Biomarkers on Polyaniline Coated Filter Paper," *IEEE Sens. J.*, vol. 17, no. 16, pp. 5021–5029, Aug. 2017, doi: 10.1109/JSEN.2017.2717701.

[87] A. Pal, V. G. Nadiger, D. Goswami, and R. V. Martinez, "Conformal, waterproof electronic decals for wireless monitoring of sweat and vaginal pH at the point-of-care," *Biosens. Bioelectron.*, vol. 160, p. 112206, Apr. 2020, doi: 10.1016/j.bios.2020.112206.

[88] S. Taccola *et al.*, "Toward the use of temporary tattoo electrodes for impedancemetric respiration monitoring and other electrophysiological recordings on skin," *Sensors*, vol. 21, no. 1197, pp. 1–17, Feb. 2021, doi: 10.3390/s21041197.

[89] V. Mihajlovic, S. Patki, and J. Xu, "Noninvasive Wearable Brain Sensing," *IEEE Sens. J.*, vol. 18, no. 19, pp. 7860–7867, Oct. 2018, doi: 10.1109/JSEN.2018.2844174.

[90] P. A. Lopes *et al.*, "Soft Bioelectronic Stickers: Selection and Evaluation of Skin-Interfacing Electrodes," *Adv. Healthc. Mater.*, vol. 8, no. 1900234, pp. 1–11, Jul. 2019, doi: 10.1002/adhm.201900234.

[91] J. J. Kim and T. L. Andrew, "Real-time and noninvasive detection of UV-Induced deep tissue damage using electrical tattoos," *Biosens. Bioelectron.*, vol. 150, p. 111909, Nov. 2020, doi: 10.1016/j.bios.2019.111909.

[92] Y. T. Li, C. W. Peng, L. T. Chen, W. S. Lin, C. H. Chu, and J. J. J. Chen, "Application of implantable wireless biomicrosystem for monitoring nerve impedance of rat after sciatic nerve injury," *IEEE Trans. Neural Syst. Rehabil. Eng.*, vol. 21, no. 1, pp. 121–128, Jan. 2013, doi: 10.1109/TNSRE.2012.2219883.

[93] C. Baek, J. Kim, Y. Lee, and J. M. Seo, "Fabrication and Evaluation of Cyclic Olefin Copolymer Based Implantable Neural Electrode," *IEEE Trans. Biomed. Eng.*, vol. 67, no. 9, pp. 2542–2551, Sep. 2020, doi: 10.1109/TBME.2020.2963992.

[94] C. N. Kotanen and A. Guiseppi-Elie, "Characterization of a wireless potentiostat for integration with a novel implantable biotransducer," *IEEE Sens. J.*, vol. 14, no. 3, pp. 768–776, Mar. 2014, doi: 10.1109/JSEN.2013.2288059.

[95] B. Srinivasan and S. Tung, "Development and Applications of Portable Biosensors," *J. Lab. Autom.*, vol. 20, no. 4, pp. 365–389, Aug. 2015, doi: 10.1177/2211068215581349.

[96] J. Kim *et al.*, "Noninvasive Alcohol Monitoring Using a Wearable Tattoo-Based Iontophoretic-Biosensing System," *ACS Sensors*, vol. 1, no. 8, pp. 1011–1019, Aug. 2016, doi: 10.1021/acssensors.6b00356.

[97] A. Bratov *et al.*, "Three-dimensional interdigitated electrode array as a transducer for label-free biosensors," *Biosens. Bioelectron.*, vol. 24, no. 4, pp. 729–735, Dec. 2008, doi: 10.1016/j.bios.2008.06.057.

[98] A. K. Okyay *et al.*, "Using nanogap in label-free impedance based electrical biosensors to overcome electrical double layer effect," *Microsyst. Technol.*, vol. 23, no. 4, pp. 889–897, Apr. 2017, doi: 10.1007/s00542-015-2764-4.

[99] J. Park, Y. Lee, Y. Hwang, and S. Cho, "Interdigitated and Wave-Shaped Electrode-Based Capacitance Sensor for Monitoring Antibiotic Effects," *Sensors*, vol. 20, no. 18, p. 5237, Sep. 2020, doi: 10.3390/s20185237.

[100] H. L. Gomes, R. B. Leite, R. Afonso, P. Stallinga, and M. L. Cancela, "A microelectrode impedance method to measure interaction of cells," in *IEEE Sensors*, Oct. 2004, vol. 2, pp. 1011–1013, doi: 10.1109/ICSENS.2004.1426344.

[101] K. Dudzinski, M. Dawgul, K. D. Pluta, B. Wawro, W. Torbicz, and D. G. Pijanowska, "Spiral Concentric Two Electrode Sensor Fabricated by Direct Writing for Skin Impedance Measurements," *IEEE Sens. J.*, vol. 17, no. 16, pp. 5306–5314, Aug. 2017, doi: 10.1109/JSEN.2017.2719001.

[102] G. Kang, S. K. Yoo, H.-I. Kim, and J.-H. Lee, "Differentiation Between Normal and Cancerous Cells at the Single Cell Level Using 3-D Electrode Electrical Impedance Spectroscopy," *IEEE Sens. J.*, vol. 12, no. 5, pp. 1084–1089, May 2012, doi: 10.1109/JSEN.2011.2167227.

[103] L. F. E. Huerta-Nuñez *et al.*, "A biosensor capable of identifying low quantities of breast cancer cells by electrical impedance spectroscopy," *Sci. Rep.*, vol. 9, no. 1, p. 6419, Apr. 2019, doi: 10.1038/s41598-019-42776-9.

[104] D. Sankhala, S. Muthukumar, and S. Prasad, "A Four-Channel Electrical Impedance Spectroscopy Module for Cortisol Biosensing in Sweat-Based Wearable Applications," *SLAS Technol.*, vol. 23, no. 6, pp. 529–539, Dec. 2018, doi: 10.1177/2472630318759257.

[105] B. Kashyap, C. K. Sestok, A. G. Dabak, S. Ramaswamy, and R. Kumar, "Ultra-Precision Liquid Level Sensing Using Impedance Spectroscopy and Data Analytics," *IEEE Sens. J.*, vol. 19, no. 20, pp. 9468–9478, Oct. 2019, doi: 10.1109/JSEN.2019.2925788.

[106] M. Abdolahad, H. Shashaani, M. Janmaleki, and S. Mohajerzadeh, "Silicon nanograss based impedance biosensor for label free detection of rare metastatic cells among primary cancerous colon cells, suitable for more accurate cancer staging," *Biosens. Bioelectron.*, vol. 59, pp. 151–159, Mar. 2014, doi: 10.1016/j.bios.2014.02.079.

[107] C. R. Chaudhuri and D. Mondal, "Electrode design improvement for impedance evaluation of biological cell culture under variable frequency low intensity sinusoidal electric field," *IEEE Trans. Dielectr. Electr. Insul.*, vol. 20, no. 2, pp. 382–390, Apr. 2013, doi: 10.1109/TDEI.2013.6508738.

[108] M. Guermazi, O. Kanoun, and N. Derbel, "Investigation of Long Time Beef and Veal Meat Behavior by Bioimpedance Spectroscopy for Meat Monitoring," *IEEE Sens. J.*, vol. 14, no. 10, pp. 3624–3630, Oct. 2014, doi: 10.1109/JSEN.2014.2328858.

[109] V. C. Rodrigues *et al.*, "Electrochemical and optical detection and machine learning applied to images of genosensors for diagnosis of prostate cancer with the biomarker PCA3," *Talanta*, vol. 222, p. 121444, Jan. 2021, doi: 10.1016/j.talanta.2020.121444.

[110] A. C. Soares, J. C. Soares, V. C. Rodrigues, O. N. Oliveira, and L. H. Capparelli Mattoso, "Controlled molecular architectures in microfluidic immunosensors for detecting Staphylococcus aureus," *Analyst*, vol. 145, no. 18, pp. 6014–6023, Aug. 2020, doi: 10.1039/D0AN00714E.

[111] J. Cabrita, A. Viana, and L. Abrantes, "Copper Protection by Phosphonic Acid Self-Assembled Monolayers," *Corrosão e Protecção Mater.*, vol. 29, no. 4, pp. 114–119, Jan. 2010, [Online]. Available: https://www.researchgate.net/publication/216826536%0ACopper.

[112] O. N. Oliveira, R. M. Iost, J. R. Siqueira, F. N. Crespilho, and L. Caseli, "Nanomaterials for diagnosis: Challenges and applications in smart devices based on molecular recognition," *ACS Appl. Mater. Interfaces*, vol. 6, no. 17, pp. 14745–14766, Jun. 2014, doi: 10.1021/am5015056.

[113] A. N. Mallya and P. C. Ramamurthy, "Conjugated Molecule Based Sensor for Microbial Detection in Water with E. coli as a Case Study and Elucidation of Interaction Mechanism," *Electroanalysis*, vol. 30, no. 6, pp. 1172–1183, Jun. 2018, doi: 10.1002/elan.201800052.

[114] P. H. B. Aoki *et al.*, "Molecularly Designed Layer-by-Layer (LbL) Films to Detect Catechol Using Information Visualization Methods," *Langmuir*, vol. 29, no. 24, pp. 7542–7550, Jun. 2013, doi: 10.1021/la304544d.

[115] S. L. Swisher *et al.*, "Impedance sensing device enables early detection of pressure ulcers in vivo," *Nat. Commun.*, vol. 6, no. 1, p. 6575, Mar. 2015, doi: 10.1038/ncomms7575.

[116] Z. Chen, Y. Yang, and P.-O. Bagnaninchi, "Hybrid Learning-Based Cell Aggregate Imaging With Miniature Electrical Impedance Tomography," *IEEE Trans. Instrum. Meas.*, vol. 70, pp. 1–10, Nov. 2021, doi: 10.1109/TIM.2020.3035384.

[117] Y. Yang, J. Jia, S. Smith, N. Jamil, W. Gamal, and P.-O. Bagnaninchi, "A Miniature Electrical Impedance Tomography Sensor and 3-D Image Reconstruction for Cell Imaging," *IEEE Sens. J.*, vol. 17, no. 2, pp. 514–523, Jan. 2017, doi: 10.1109/JSEN.2016.2631263.

[118] C. Zhang *et al.*, "An Impedance Sensing Platform for Monitoring Heterogeneous Connectivity and Diagnostics in Lab-on-a-Chip Systems," *ACS Omega*, vol. 5, no. 10, pp. 5098–5104, Mar. 2020, doi: 10.1021/acsomega.9b04048.

[119] J. S. Park *et al.*, "1024-Pixel CMOS Multimodality Joint Cellular Sensor/Stimulator Array for Real-Time Holistic Cellular Characterization and Cell-Based Drug Screening," *IEEE Trans. Biomed. Circuits Syst.*, vol. 12, no. 1, pp. 80–94, Feb. 2018, doi: 10.1109/TBCAS.2017.2759220.

[120] T. S. Pui *et al.*, "High density CMOS electrode array for high-throughput and automated cell counting," *Sensors Actuators B Chem.*, vol. 181, pp. 842–849, May 2013, doi: 10.1016/j.snb.2013.02.065.

[121] N. Ogata *et al.*, "An Electrical Impedance Biosensor Array for Tracking Moving Cells," in *2018 IEEE SENSORS*, Oct. 2018, pp. 1–4, doi: 10.1109/ICSENS.2018.8589577.

[122] Kyomuk Lim, Jindeok Seo, Changho Seok, and Hyoungho Ko, "A 16-channel neural stimulator with DAC sharing scheme for visual prostheses," in *IEEE International Symposium on Circuits and Systems*, May 2013, vol. 2, pp. 1873–1876, doi: 10.1109/ISCAS.2013.6572231.

[123] Z. Hu, R. Ramalingame, A. Y. Kallel, F. Wendler, Z. Fang, and O. Kanoun, "Calibration of an AC Zero Potential Circuit for Two-Dimensional Impedimetric Sensor Matrices," *IEEE Sens. J.*, vol. 20, no. 9, pp. 5019–5025, May 2020, doi: 10.1109/JSEN.2020.2966141.

[124] Y.-Y. Lu, J.-J. Huang, Y.-J. Huang, and K.-S. Cheng, "Cell growth characterization using multi-electrode bioimpedance spectroscopy," *Meas. Sci. Technol.*, vol. 24, no. 3, p. 035701, Jan. 2013, doi: 10.1088/0957-0233/24/3/035701.

[125] J. Chung, Y. Chen, and S.-J. Kim, "High-density impedance-sensing array on complementary metal-oxide-semiconductor circuitry assisted by negative dielectrophoresis for single-cell-resolution measurement," *Sensors Actuators B Chem.*, vol. 266, pp. 106–114, Aug. 2018, doi: 10.1016/j.snb.2018.03.113.

[126] F. Widdershoven *et al.*, "A CMOS Pixelated Nanocapacitor Biosensor Platform for High-Frequency Impedance Spectroscopy and Imaging," *IEEE Trans. Biomed. Circuits Syst.*, vol. 12, no. 6, pp. 1369–1382, Dec. 2018, doi: 10.1109/TBCAS.2018.2861558.

[127] Z. Jiang *et al.*, "Development of a Portable Electrochemical Impedance Spectroscopy System for Bio-Detection," *IEEE Sens. J.*, vol. 19, no. 15, pp. 5979–5987, Aug. 2019, doi: 10.1109/JSEN.2019.2911718.

[128] H. P. Schwan, "Linear and nonlinear electrode polarization and biological materials," *Ann. Biomed. Eng.*, vol. 20, no. 3, pp. 269–288, May 1992, doi: 10.1007/BF02368531.

[129] M. Z. Bazant, K. Thornton, and A. Ajdari, "Diffuse-charge dynamics in electrochemical systems," *Phys. Rev. E*, vol. 70, no. 2, p. 021506, Aug. 2004, doi: 10.1103/PhysRevE.70.021506.

[130] Z. Zou, J. Kai, M. J. Rust, J. Han, and C. H. Ahn, "Functionalized nano interdigitated electrodes arrays on polymer with integrated microfluidics for direct bio-affinity sensing using impedimetric measurement," *Sensors Actuators A Phys.*, vol. 136, no. 2, pp. 518–526, May 2007, doi: 10.1016/j.sna.2006.12.006.

[131] A. Bonanni, I. Fernández-Cuesta, X. Borrisé, F. Pérez-Murano, S. Alegret, and M. del Valle, "DNA hybridization detection by electrochemical impedance spectroscopy using interdigitated gold nanoelectrodes," *Microchim. Acta*, vol. 170, no. 3–4, pp. 275–281, Sep. 2010, doi: 10.1007/s00604-010-0358-5.

[132] J. Claudel, A. L. Alves De Araujo, M. Nadi, and D. Kourtiche, "Lab-On-A-Chip Device for Yeast Cell Characterization in Low-Conductivity Media Combining Cytometry and Bio-Impedance," *Sensors*, vol. 19, no. 15, p. 3366, Jul. 2019, doi: 10.3390/s19153366.

[133] A. L. Alves de Araujo, J. Claudel, D. Kourtiche, and M. Nadi, "Influence of Electrode Connection Tracks on Biological Cell Measurements by Impedance Spectroscopy," *Sensors*, vol. 19, no. 13, p. 2839, Jun. 2019, doi: 10.3390/s19132839.

[134] K. F. Lei and P. H. M. Leung, "Microelectrode array biosensor for the detection of Legionella pneumophila," *Microelectron. Eng.*, vol. 91, pp. 174–177, Mar. 2012, doi: 10.1016/j.mee.2011.10.002.

[135] D. Sticker *et al.*, "Zirconium dioxide nanolayer passivated impedimetric sensors for cell-based assays," *Sensors Actuators B Chem.*, vol. 213, pp. 35–44, Jul. 2015, doi: 10.1016/j.snb.2015.02.018.

[136] A. Riul Jr., C. A. R. Dantas, C. M. Miyazaki, and O. N. Oliveira Jr., "Recent advances in electronic tongues," *Analyst*, vol. 135, no. 10, p. 2481, Aug. 2010, doi: 10.1039/c0an00292e.

[137] B. H. Zhang, R. H. Wang, Y. X. Wang, and Y. Bin Li, "LabVIEW-based impedance biosensing system for detection of avian influenza virus," *Int. J. Agric. Biol. Eng.*, vol. 9, no. 4, pp. 116–122, Jul. 2016, doi: 10.3965/j.ijabe.20160904.1704.

[138] N. Das, N. Samanta, and C. R. Chaudhuri, "Nanostructured Silicon Oxide Immunosensor Integrated with Noise Spectroscopy Electronics for POC Diagnostics," in *29th International Conference on VLSI Design*, Jan. 2016, pp. 367–372, doi: 10.1109/VLSID.2016.53.

[139] A. C. Soares *et al.*, "Microfluidic-Based Genosensor To Detect Human Papillomavirus (HPV16) for Head and Neck Cancer," *ACS Appl. Mater. Interfaces*, vol. 10, no. 43, pp. 36757–36763, Oct. 2018, doi: 10.1021/acsami.8b14632.

[140] H. Wu *et al.*, "A polyaniline-modified immunosensor based on four-wire interdigitated microelectrode," *J. Micro-Bio Robot.*, vol. 12, no. 1–4, pp. 1–8, Jun. 2017, doi: 10.1007/s12213-016-0093-z.

[141] R. B. Queirós, N. De-los-Santos-Álvarez, J. P. Noronha, and M. G. F. Sales, "A label-free DNA aptamer-based impedance biosensor for the detection of E. coli outer membrane proteins," *Sensors Actuators B Chem.*, vol. 181, pp. 766–772, May 2013, doi: 10.1016/j.snb.2013.01.062.

[142] K. Jiang *et al.*, "Rapid label-free detection of E. coli using antimicrobial peptide assisted impedance spectroscopy," *Anal. Methods*, vol. 7, no. 23, pp. 9744–9748, Aug. 2015, doi: 10.1039/C5AY01917F.

[143] O. Estrada-Leypon *et al.*, "Simultaneous monitoring of Staphylococcus aureus growth in a multi-parametric microfluidic platform using microscopy and impedance spectroscopy," *Bioelectrochemistry*, vol. 105, pp. 56–64, Oct. 2015, doi: 10.1016/j.bioelechem.2015.05.006.

[144] D. Wilson, E. M. Materón, G. Ibáñez-Redín, R. C. Faria, D. S. Correa, and O. N. Oliveira, "Electrical detection of pathogenic bacteria in food samples using information visualization methods with a sensor based on magnetic nanoparticles functionalized with antimicrobial peptides," *Talanta*, vol. 194, pp. 611–618, Mar. 2019, doi: 10.1016/j.talanta.2018.10.089.

[145] J. Paredes, S. Becerro, F. Arizti, A. Aguinaga, J. L. Del Pozo, and S. Arana, "Interdigitated microelectrode biosensor for bacterial biofilm growth monitoring by impedance spectroscopy technique in 96-well microtiter plates," *Sensors Actuators B Chem.*, vol. 178, pp. 663–670, Mar. 2013, doi: 10.1016/j.snb.2013.01.027.

[146] N. Pal, S. Sharma, and S. Gupta, "Sensitive and rapid detection of pathogenic bacteria in small volumes using impedance spectroscopy technique," *Biosens. Bioelectron.*, vol. 77, pp. 270–276, Sep. 2016, doi: 10.1016/j.bios.2015.09.037.

[147] I. Tubía, J. Paredes, E. Pérez-Lorenzo, and S. Arana, "Antibody biosensors for spoilage yeast detection based on impedance spectroscopy," *Biosens. Bioelectron.*, vol. 102, pp. 432–438, Apr. 2018, doi: 10.1016/j.bios.2017.11.057.

[148] J. B. M. Rocha Neto *et al.*, "Polysaccharide Multilayer Films in Sensors for Detecting Prostate Tumor Cells Based on Hyaluronan-CD44 Interactions," *Cells*, vol. 9, no. 6, p. 1563, Jun. 2020, doi: 10.3390/cells9061563.

[149] A. C. Soares, J. C. Soares, F. M. Shimizu, M. E. Melendez, A. L. Carvalho, and O. N. Oliveira, "Controlled Film Architectures to Detect a Biomarker for Pancreatic Cancer Using Impedance Spectroscopy," *ACS Appl. Mater. Interfaces*, vol. 7, no. 46, pp. 25930–25937, Nov. 2015, doi: 10.1021/acsami.5b08666.

[150] A. C. Soares *et al.*, "A simple architecture with self-assembled monolayers to build immunosensors for detecting the pancreatic cancer biomarker CA19-9," *Analyst*, vol. 143, no. 14, pp. 3302–3308, Apr. 2018, doi: 10.1039/C8AN00430G.

[151] J. C. Soares *et al.*, "Immunosensor for Pancreatic Cancer Based on Electrospun Nanofibers Coated with Carbon Nanotubes or Gold Nanoparticles," *ACS Omega*, vol. 2, no. 10, pp. 6975–6983, Oct. 2017, doi: 10.1021/acsomega.7b01029.

[152] G. Soraya *et al.*, "A Label-Free, Quantitative Fecal Hemoglobin Detection Platform for Colorectal Cancer Screening," *Biosensors*, vol. 7, no. 4, p. 19, May 2017, doi: 10.3390/bios7020019.

[153] J. Yun, Y.-T. Hong, K.-H. Hong, and J.-H. Lee, "Ex vivo identification of thyroid cancer tissue using electrical impedance spectroscopy on a needle," *Sensors Actuators B Chem.*, vol. 261, pp. 537–544, May 2018, doi: 10.1016/j.snb.2018.01.155.

[154] R. F. Kushner, "Bioelectrical Impedance Analysis: A Review of Principles and Applications," *J. Am. Coll. Nutr.*, vol. 11, no. 2, pp. 199–209, Apr. 1992, doi: 10.1080/07315724.1992.12098245.

[155] M. L. Moraes *et al.*, "Immobilization of cholesterol oxidase in LbL films and detection of cholesterol using ac measurements," *Mater. Sci. Eng. C*, vol. 29, no. 2, pp. 442–447, Mar. 2009, doi: 10.1016/j.msec.2008.08.040.

[156] M. L. Moraes *et al.*, "Detection of glucose and triglycerides using information visualization methods to process impedance spectroscopy data," *Sensors Actuators B Chem.*, vol. 166–167, pp. 231–238, May 2012, doi: 10.1016/j.snb.2012.02.046.

[157] C. Garcia-Hernandez, C. Salvo Comino, F. Martín-Pedrosa, M. L. Rodriguez-Mendez, and C. Garcia-Cabezon, "Impedimetric electronic tongue based on nanocomposites for the analysis of red wines. Improving the variable selection method," *Sensors Actuators B Chem.*, vol. 277, pp. 365–372, Dec. 2018, doi: 10.1016/j.snb.2018.09.023.

[158] Y. Elamine *et al.*, "Insight into the sensing mechanism of an impedance based electronic tongue for honey botanic origin discrimination," *Sensors Actuators B Chem.*, vol. 285, pp. 24–33, Apr. 2019, doi: 10.1016/j.snb.2019.01.023.

[159] A. Riul, R. R. Malmegrim, F. J. Fonseca, and L. H. C. Mattoso, "An artificial taste sensor based on conducting polymers," *Biosens. Bioelectron.*, vol. 18, no. 11, pp. 1365–1369, Oct. 2003, doi: 10.1016/S0956-5663(03)00069-1.

[160] P. Ibba, A. Falco, A. Rivadeneyra, and P. Lugli, "Low-Cost Bio-Impedance Analysis System for the Evaluation of Fruit Ripeness," in *2018 IEEE SENSORS*, Oct. 2018, pp. 1–4, doi: 10.1109/ICSENS.2018.8589541.

[161] M. H. M. Facure, L. A. Mercante, L. H. C. Mattoso, and D. S. Correa, "Detection of trace levels of organophosphate pesticides using an electronic tongue based on graphene hybrid nanocomposites," *Talanta*, vol. 167, pp. 59–66, May 2017, doi: 10.1016/j.talanta.2017.02.005.

[162] Y. Chen *et al.*, "CMOS high density electrical impedance biosensor array for tumor cell detection," *Sensors Actuators B Chem.*, vol. 173, pp. 903–907, Oct. 2012, doi: 10.1016/j.snb.2012.07.024.

[163] F. Cui, Y. Yue, Y. Zhang, Z. Zhang, and H. S. Zhou, "Advancing

Biosensors with Machine Learning," *ACS Sensors*, vol. 5, no. 11, pp. 3346–3364, Nov. 2020, doi: 10.1021/acssensors.0c01424.

[164] S. Lekha and S. M, "Recent Advancements and Future Prospects on E-Nose Sensors Technology and Machine Learning Approaches for Non-Invasive Diabetes Diagnosis: A Review," *IEEE Rev. Biomed. Eng.*, vol. 14, pp. 127–138, May 2021, doi: 10.1109/RBME.2020.2993591.

[165] M. J. Adams, *Chemometrics in Analytical Spectroscopy*. Cambridge, UK: The Royal Society of Chemistry, 1995.

[166] Americo da Silva, Braunger, Neris Coutinho, Rios do Amaral, Rodrigues, and Riul Jr., "3D-Printed Graphene Electrodes Applied in an Impedimetric Electronic Tongue for Soil Analysis," *Chemosensors*, vol. 7, no. 4, p. 50, Oct. 2019, doi: 10.3390/chemosensors7040050.

[167] A. K. Gupta *et al.*, "Label-Free Electrochemical Detection of Dibenzofuran Using MnO_2 Nanofibres," *IEEE Sens. J.*, vol. 20, no. 21, pp. 12537–12542, Nov. 2020, doi: 10.1109/JSEN.2020.3002158.

[168] O. N. Oliveira, F. J. Pavinatto, C. J. L. Constantino, F. V. Paulovich, and M. C. F. de Oliveira, "Information Visualization to Enhance Sensitivity and Selectivity in Biosensing," *Biointerphases*, vol. 7, no. 1, p. 53, Dec. 2012, doi: 10.1007/s13758-012-0053-7.

[169] C. Magro *et al.*, "Polyelectrolyte Based Sensors as Key to Achieve Quantitative Electronic Tongues: Detection of Triclosan on Aqueous Environmental Matrices," *Nanomaterials*, vol. 10, no. 4, p. 640, Mar. 2020, doi: 10.3390/nano10040640.

[170] M. Braunger *et al.*, "Microfluidic Electronic Tongue Applied to Soil Analysis," *Chemosensors*, vol. 5, no. 2, p. 14, Apr. 2017, doi: 10.3390/chemosensors5020014.

[171] J. C. Soares *et al.*, "Adsorption according to the Langmuir–Freundlich model is the detection mechanism of the antigen p53 for early diagnosis of cancer," *Phys. Chem. Chem. Phys.*, vol. 18, no. 12, pp. 8412–8418, Feb. 2016, doi: 10.1039/C5CP07121F.

[172] A. L. Meyrowitz and S. Chipman, *Foundations of Knowledge Acquisition: Machine Learning*. Norwell, USA: Kluwer Academic Publishers, 1993.

[173] A. Banerjee, S. Maity, and C. H. Mastrangelo, "Nanostructures for Biosensing, with a Brief Overview on Cancer Detection, IoT, and the Role of Machine Learning in Smart Biosensors," *Sensors*, vol. 21, no. 4, p. 1253, Feb. 2021, doi: 10.3390/s21041253.

[174] E. J. Ferreira, R. C. T. Pereira, A. C. B. Delbem, O. N. Oliveira, and L. H. C. Mattoso, "Random subspace method for analysing coffee with electronic tongue," *Electron. Lett.*, vol. 43, no. 21, p. 1138, Oct. 2007, doi: 10.1049/el:20071182.

[175] A. B. Cunha, J. Hou, and C. Schuelke, "Machine learning for stem cell differentiation and proliferation classification on electrical impedance spectroscopy," *J. Electr. Bioimpedance*, vol. 10, no. 1, pp. 124–132, Dec. 2019, doi: 10.2478/joeb-2019-0018.

[176] W. A. Christinelli *et al.*, "Two-dimensional MoS2-based impedimetric electronic tongue for the discrimination of endocrine disrupting chemicals using machine learning," *Sensors Actuators B Chem.*, vol. 336, p. 129696, Jun. 2021, doi: 10.1016/j.snb.2021.129696.

[177] M. Tiitta, V. Tiitta, J. Heikkinen, R. Lappalainen, and L. Tomppo, "Classification of Wood Chips Using Electrical Impedance Spectroscopy and Machine Learning," *Sensors*, vol. 20, no. 4, p. 1076, Feb. 2020, doi: 10.3390/s20041076.

Lorenzo A. Buscaglia was born in San Carlos de Bariloche, Argentina. He received his B.S. degree in mechatronics engineering from the University of São Paulo, São Carlos, Brazil, in 2018. He is currently pursuing the M.S. degree in applied physics, with computational emphasis, at the same university. His research interest includes the development of low-cost devices for sensing and biosensing applications, being specialized in the electrical impedance spectroscopy techniques.

Osvaldo N. Oliveira Jr. is a professor at the São Carlos Institute of Physics, University of São Paulo, Brazil, having obtained his PhD from Bangor University in 1990. He is a member of the Latin American Academy of Sciences and Brazilian Academy of Sciences, First-vice president of the International Union of Materials Research Society (IUMRS), and executive editor of ACS Applied Materials & Interfaces. Prof. Oliveira has led research into novel materials and has pioneered the combined use of statistical physics and artificial intelligence to process text and analyze sensing and biosensing data.

João Paulo Carmo was born in Maia, Portugal, in 1970. He is Professor at the University of São Paulo (USP), São Carlos, Brazil. He is involved in the research on micro/nano-technologies, solid-state integrated sensors, and microdevices for biomedical and industrial applications. Professor Carmo is also Vice-Director of the Group of Metamaterials, Microwaves and Optics (GMeta).